RAPID COMMUNICATIONS

PHYSICAL REVIEW B VOLUME 28, NUMBER 9 1 NOVEMBER 1983

Rapid Communications

The Rapid Communications section is intended for the accelerated publication of important new results. Manuscripts submitted to this section are given priority in handling in the editorial office and in production. A Rapid Communication may be no longer than 3½ printed pages and must be accompanied by an abstract. Page proofs are sent to authors, but, because of the rapid publication schedule, publication is not delayed for receipt of corrections unless requested by the author.

Angle-resolved photoemission and secondary electron emission from single-crystal graphite

A. R. Law, J. J. Barry, and H. P. Hughes

Surface Physics Group, Cavendish Laboratory, Madingley Road, Cambridge CB3 OHE, United Kingdom

(Received 20 May 1983; revised manuscript received 25 July 1983)

Angle-resolved photoemission from a single crystal of natural graphite is reported for the first time. The absence of turbostratic disorder allows unambiguous determination of the valence-band dispersions in the two principal symmetry directions. Other features observed in photoemission, and in electron-excited angle-resolved secondary electron emission, are attributed to conduction-band states, and allow conduction-band dispersions to be measured directly.

The band structure of graphite has been the subject of much experimental and theoretical study. Graphite is the archetypal layered material with strong intralayer σ bonds based on the sp^2 hybridized atomic $2s$, $2p_x$, and $2p_y$ orbitals and weak interlayer π bonding originating from the $2p_z$ orbitals. This layered structure facilitates theoretical calculations of the band structure and many computational techniques have been employed.[1]

The two-dimensional morphology also makes graphite particularly amenable to study by angle-resolved ultraviolet photoemission (ARUPS), and we present here polar and azimuthal ARUPS data for a single crystal of natural graphite using He I and He II incident radiation. Angle-resolved secondary electron emission is also examined, and our results are compared with the recent three-dimensional *ab initio* band-structure calculation of Tatar and Rabii.[1]

ARUPS data from highly oriented pyrolytic graphite (HOPG) reported by Williams[2] show dispersion of features in the valence band consistent with that calculated by Painter and Ellis[3]: A detailed comparison with theory is impossible because of the turbostratically disordered nature of HOPG, resulting in averaging of the photocurrent over all crystal azimuths. More recently, McGovern, Eberhardt, Plummer, and Fischer[4] have performed synchrotron radiation-excited ARUPS, again from HOPG, which for off-normal emission showed noticeable variation with azimuthal orientation ϕ of the sample; some azimuthal ordering was also apparent in electron diffraction. Their mapping of the valence bands, however, seems insufficiently distinct to allow a definite interpretation of the anisotropy observed in terms of the ϕ variation predicted for a single crystal.

We report experiments performed in an ultrahigh vacuum system using a standard gas discharge light source, unpolarized, operating at both He I (21.2 eV) and He II (40.8 eV). The photoelectrons were energy analyzed using a hemispherical sector analyzer movable around the sample in a horizontal plane only, having angular acceptance $\pm 2°$ and energy resolution ≈ 0.2 eV. The sample of Ticonderoga graphite was freshly cleaved prior to insertion into the vacuum system and subsequently cleaned *in situ* by electron bombardment heating to $\geq 1500\,°C$. Several samples were investigated before one showing satisfactorily sharp low-energy electron diffraction (LEED) over a usable area was found. These good LEED patterns confirmed the monocrystalline nature of the sample and allowed unambiguous determination of the azimuthal orientation.

Figure 1 shows the energy distribution curves (EDC's) measured in the ΓAHK and ΓALM azimuths using He I light incident at 45° (i.e., mixed "*s*" and "*p*" polarization). The dominant feature in both sets of spectra is the strong peak moving towards the Fermi energy E_F as the polar angle ϕ increases. The ΓAHK spectra also show a prominent feature moving downwards from E_F for $\phi > 20°$.

In Fig. 2 the observed features are reduced, in the usual way,[5] to an initial-state energy versus parallel component of momentum (E_i vs $k_\parallel$) diagram. Superimposed on the experimental data are the initial-state bands of the Korringa-Kohn-Rostoker (KKR) calculation of Tatar and Rabii[1] for the ΓMK plane of the Brillouin zone BZ. The theoretical bands have been rigidly shifted down in energy by 0.5 eV to give the best qualitative agreement with the experimental band positions and dispersions. The necessity for this shift may be the result of donor impurities raising the Fermi level up through the conduction band. The density of states near E_F is small (1.2×10^{-4} states per carbon atom per eV) so only a very small concentration of impurities—around 0.01 at.%—would be required to give the observed shift: Such a low concentration would not be observed by x-ray photoelectron surface chemical analysis.

From Fig. 2 the strong peak in the EDC's is now readily identifiable as the π valence band. Theory predicts a π-band splitting of ≈ 1 eV in the ΓMK plane of the BZ because of layer-layer interactions. This is not resolved here since the photocurrent is effectively an average over the BZ in the ΓA direction. Lifetime broadening in the initial state may also smear out any fine structure. The other strong feature in the EDC's for the ΓAHK plane corresponds to the σ valence bands. The π-band/σ-band intensity ratio

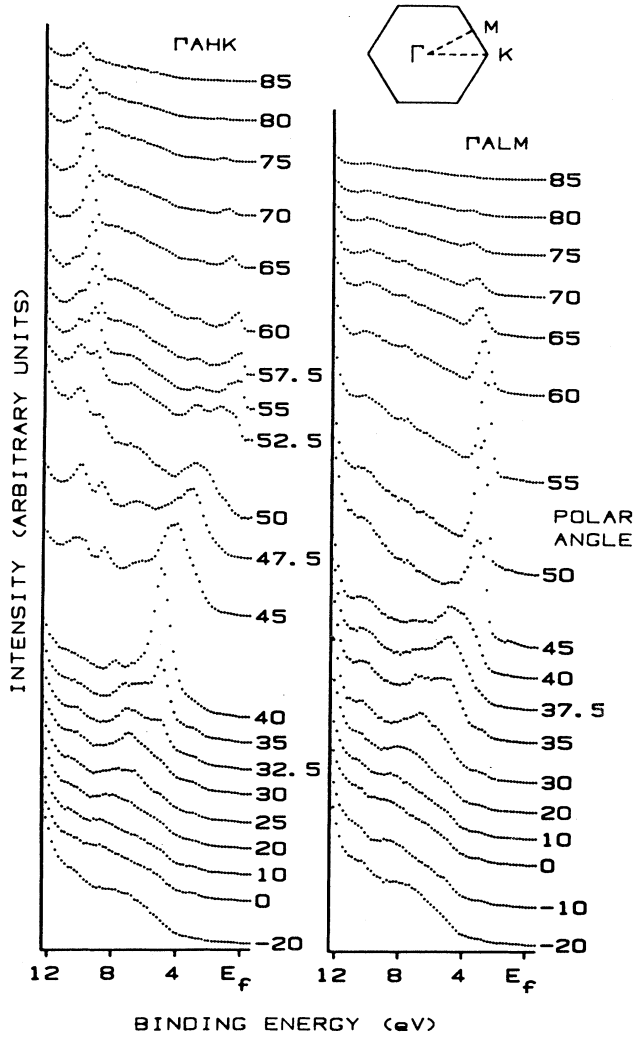

FIG. 1. EDC's for the Γ*AHK* and Γ*ALM* planes of graphite obtained using mixed-polarization He I. The spectra have been truncated to facilitate display and do not show features with binding energies > 12 eV.

drops off as ϕ is increased, reflecting the expected polar variation for the parent atomic orbitals.

The predicted σ bands near $\Gamma(A)$ do not appear in the He I spectra of Fig. 1 but are observed using He II radiation. For He I radiation there are no final electron states accessible by direct transitions at the appropriate energy, so the photoexcitation cross section is very small.

σ-band features in the Γ*ALM* plane are weaker than those in the Γ*AHK* plane. This suppression of σ bands can be explained by a detailed consideration of both the initial and final states concerned. As pointed out by Hermanson,[6] photoelectrons can be detected only if the final-state electron wave function within the solid can match onto a free-electron (plane wave) wave function with finite amplitude at the detector: in the case of detection in a mirror plane of the crystal, this means only final states even under reflection in this mirror plane. The Γ*ALM* plane of graphite corresponds to a mirror plane in real space whereas Γ*AHK*

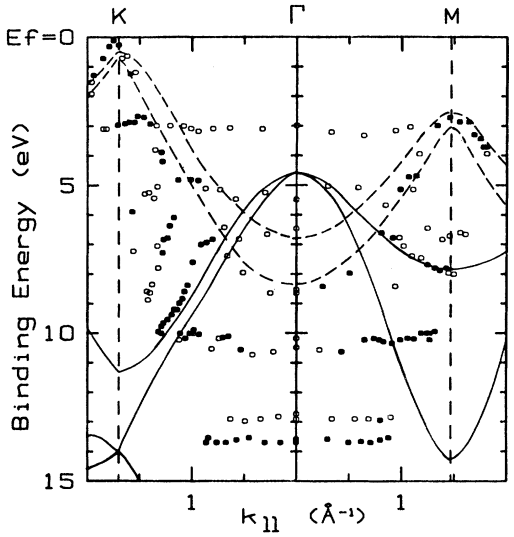

FIG. 2. Binding energies of features in the EDC's, plotted against $k_{\parallel}$ (●, strong or distinct features; ○, weak features) compared with theoretical valence bands (Ref. 1). Dashed curves are π bands, continuous curves are σ bands.

does not: Thus the highly dispersive final state in the Γ*ALM* plane (labeled as Σ_4 in Fig. 3), which is odd under reflection in this plane, cannot be observed in photoemission, even if transitions to it are optically allowed.

The lower binding energy σ band is observed weakly at

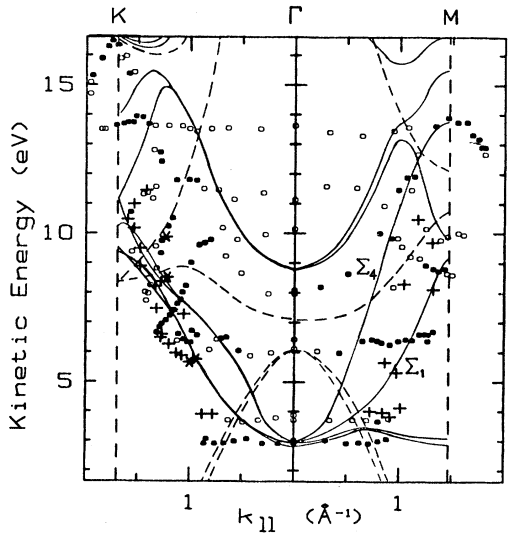

FIG. 3. Kinetic energy above the vacuum level of features in He I photoemission EDC's, plotted against $k_{\parallel}$ (●, strong or distinct features; ○, weak features). Also shown are electron-excited secondary electron features (*, strong features, +, weak features). Continuous curves are theoretical σ^* conduction bands and dashed curves are π^* bands (Ref. 1). For reasons of clarity the strong feature at ≈ 3 eV kinetic energy seen in electron-excited SEE is not plotted, but coincides with the data for photoemission. The state labeled Σ_4 is odd under reflection in the Γ*ALM* plane and will not be observed in photoemission and the interlayer state predicted by Posternak *et al.* (Ref. 12) is labeled Σ_1.

$k_{\parallel} \approx 1$ Å^{-1} for mixed polarization light but is not observed when the He I radiation is incident normal to the sample. This confirms the predicted π^* nature of the relevant final state since for the elector vector, E, perpendicular to the c axis only $\pi \leftrightarrow \pi$ and $\sigma \leftrightarrow \sigma$ transitions are allowed. The nonappearance of the higher-binding-energy valence band in the He I spectra, although transitions from it are optically allowed, is probably due to the very low joint density of states resulting from the opposite gradients of the initial and final bands.

Other features in the photoemission spectra are ascribed to secondary electrons. Figure 3 shows the data of Fig. 2 plotted on a kinetic energy E vs $k_{\parallel}$ diagram and compared with the theoretical conduction bands of Ref. 1. Unlike the valence bands, the conduction bands have not been shifted in energy: The calculated minimum in the σ^* conduction bands at Γ coincides with the strong nondispersive feature observed at ≈ 3 eV kinetic energy above the vacuum level (≈ 7.6 eV above E_F, the measured work function of the sample being 4.60 eV, in agreement with the value of 4.70 eV determined by Willis, Fitton, and Painter[7] using a Fowler plot). Our identification of structure near K at ≈ 13 eV kinetic energy, and near $\frac{2}{3}\,\Gamma K$ at ≈ 10 eV kinetic energy, as due to electrons emerging from conduction bands predicted in the regions concerned is confirmed by spectra recorded with normally incident He I light (s polarized). Under these conditions the secondary peaks are just as intense as in mixed polarization, while the primary photoelectron peaks are diminished. Also these features remain at the same kinetic energy above the vacuum level in spectra recorded with He II radiation. Perhaps better agreement with theory is achieved for these features if the calculated conduction bands are shifted down by ≈ 0.5 eV.

We have also performed angle-dispersive secondary electron emission (SEE) using electrons of incident energies ≈ 60 eV: The present experimental configuration does not allow polar emission angles of less than 40°.

Willis, Fitton, and Painter[7] have demonstrated that SEE spectra from HOPG contain strong structure associated with regions of high density of states in the conduction band. The most prominent feature in our spectra is the ≈ 3 eV kinetic energy peak and, as in photoemission, it shows no dispersion in either azimuthal direction. It has recently been suggested that accurate electron spectrometer calibration can be achieved by observation of this feature from Aquadag.[8]

Other higher-energy features, much weaker than the ≈ 3 eV peak but showing dispersion with increasing emission angle, were obtained from the first derivative of the secondary electron EDC's. Since $k_{\parallel}$ conservation applies as much to secondaries as to photoelectrons, these dispersive features have been reduced to E, $k_{\parallel}$ points, and are also plotted in Fig. 3.

As stated above, the peak at ≈ 3 eV above the vacuum level is observed not to disperse in both ARUPS and SEE. The energy of this feature corresponds to the σ^* conduction-band minimum at $\Gamma(A)$ which shows weak dispersion near ΓA, resulting in a high density of final states at this point. The calculated lowest energy σ^* band shows little dispersion in the ΓALM plane, in agreement with experiment, but in the ΓAHK plane theory predicts a dispersion upwards of the lowest σ^* band, its energy being ≈ 10 eV higher at the BZ boundary, HK, than at the zone center. Weak emission from this band is observed in the SEE spectra. We thus attribute the observation of the ≈ 3 eV feature for polar emission angles out to 90° in the ΓAHK plane to momentum broadening in the final states at ΓA. The wave vector of this feature at high emission angles is ≈ 1 Å^{-1}, being ≈ 0.5 Å^{-1} distant from the nearest predicted final states at this energy. This implies a mean free path of ≈ 5 Å, much shorter than might be expected for such low kinetic energy electrons from consideration of the "universal curve" of mean free paths versus energy.

Electrons in the σ^*-band minimum at Γ have a very high effective mass m^* in the c-axis direction along ΓA (as well as the relatively high m^* in the ΓALM plane), and hence a low group velocity. This would result in considerable scattering, a short mean free path, and substantial momentum broadening, as apparently observed. Since there are no final states below this σ^* band at Γ it will act as a "sump" for electrons scattered down from higher-energy states: This together with the high density of states may account for the strength of the feature. Other weak dispersionless structure across $K\Gamma M$ at binding energies of around 3, 5, and 10 eV can probably also be attributed to momentum broadening at regions of high densities of final states.

In conclusion, good agreement has been found, in both principal symmetry directions, between the experimental data and the KKR band-structure calculation of Tatar and Rabii[1] for both valence- and conduction-band features. Other full-band-structure calculations, using a pseudopotential approach by van Haeringen and Junginger[9] and Holzwarth, Louie and Rabii,[10] and by Mallett[11] using a cellular method, produce very similar bandwidths and dispersions, but with sizable energy shifts between bands of σ and π character. For example, Mallett's[11] calculation places the σ valence band ≈ 3 eV higher in energy with respect to the π valence band, while Refs. 9 and 10 agree more closely with Tatar and Rabii[1] with the σ band only ≈ 1 eV higher at Γ. With the exception of one conduction band to be discussed further below, all four calculations produce conduction bands of overall similarity, but again Mallett's[11] calculation places the bottom of the σ^*-band manifold ≈ 3 eV too high compared with Tatar and Rabii[1] and with our experimental data. Mallett's[11] calculation seems, therefore, consistently to place the σ-based bands ≈ 3 eV too high with respect to the π-based bands, presumably the result of the use of a spherically symmetric potential. Bearing in mind the relationship of the σ and π orbitals to the layered structure of graphite, it is reasonable to suppose that the spherical potential, rather than one reflecting the layered character of the material, would effectively overemphasize the binding energies of the out-of-plane π-orbital-based bands.

Posternak *et al.*[12] have recently demonstrated the existence of a new kind of conduction-band state in graphite, at energies close to the π^* bands, using a self-consistent local-density all-electron theory. These states exhibit free-electron character parallel to the basal plane, and have charge densities concentrated between the graphite layers. These new states are also present in the calculations of Tatar and Rabii[1] and appear as a Σ_1 state between Γ and M as indicated in Fig. 3, and in the calculations of Refs. 9, 10, and 11. Earlier linear combination of atomic orbitals calculations of the band structure of graphite based solely on the C $2s$ and $2p$ levels do not include these interlayer states, which have considerable C $3s$ character. It can be seen

from Fig. 3 that some experimental evidence for these Σ_1 conduction-band states exists, since weak features in the SEE spectra appear, corresponding to points in the appropriate region of k space, where no other conduction bands are predicted. Mallett[11] again finds this band to be ≈ 4 eV lower in energy than Tatar and Rabii,[1] so that at Γ it lies below the vacuum level and is therefore inaccessible to photoemission and SEE experiments. This discrepancy presumably arises once again from the spherical potential used by Mallett, which is likely to overestimate the binding energies of states concentrated between the layers.

ACKNOWLEDGMENT

Two of us (A.R.L. and J.J.B.) gratefully acknowledge the support of the United Kingdom Science and Engineering Research Council.

[1]R. C. Tatar and S. Rabii, Phys. Rev. B 25, 4126 (1982), and references therein.
[2]P. M. Williams, Nuovo Cimento 38B, 216 (1977).
[3]G. S. Painter and D. E. Ellis, Phys. Rev. B 1, 4747 (1970).
[4]I. T. McGovern, W. Eberhardt, E. W. Plummer, and J. E. Fischer, Physica B 99, 415 (1980).
[5]H. P. Hughes and W. Y. Liang, J. Phys. C 6, 1684 (1973).
[6]J. Hermanson, Solid State Commun. 22, 9 (1977).
[7]R. F. Willis, B. Fitton, and G. S. Painter, Phys. Rev. B 9, 1926 (1974).
[8]P. Oelhafen and J. L. Freeouf, J. Vac. Sci. Technol. A1, 96 (1983).
[9]W. van Haeringen and H.-G. Junginger, Solid State Commun. 7, 1723 (1969).
[10]N. A. W. Holzwarth, S. G. Louie, and S. Rabii, Phys. Rev. B 26, 5382 (1982).
[11]C. P. Mallett, J. Phys. C 14, L213 (1981).
[12]M. Posternak, A. Baldereschi, A. J. Freeman, E. Wimmer, and M. Weinert, Phys. Rev. Lett. 50, 761 (1983).